`

Kerbala Journal for Engineering Science

https://kjes.uokerbala.edu.iq/

Calculation of Static and Dynamic Characteristics of a Finite Length Journal Bearing Considering 3D Misalignment

Zahraa A. AL-Dujaili*, Hazim U. Jamali* and Moneer H. Tolephih**

* University of Kerbala, Karbala, Iraq

zahraa.abdul@uokerbala.edu.iq

** University of Baghdad, Baghdad, Iraq

Received: 16 June 2020; Revised: 20 August 2020; Accepted: 29 August 2020

Abstract

The main purpose of the journal bearing is to support the rotating parts by providing a sufficient layer of lubricant to separate the surfaces of the moving parts and to minimize the friction due to rotation. The misalignment is one of the common problems in the industrial applications of this type of bearing which has consequences on the general performance of the bearing system. The consequences include the reduction in the bearing load carrying capacity and the effect on the levels of the pressure distribution in additional to the asymmetrical pressure distribution along the bearing width. This study considers extreme cases of misalignment using a 3D model of the shaft deviation for the case of a finite length bearing. Numerical solution for Reynolds equation is considered in this work using the finite difference method where the static and dynamic characteristics of finite length journal bearing are investigated. The results reveal that the film thickness reduces significantly particularly at the edges of the additional to the presence of pressure spikes at these locations. Furthermore, the results of the dynamic coefficients have shown that the 3D misalignment affects these coefficients significantly which may have further consequences on the stability of the system.

***Key words*:** Journal bearing, 3D Misalignment, Dynamic and static coefficients, Numerical analysis.

`

1. Introduction

Journal bearing (J.B.) consists of two main parts, which are journal (shaft) and bearing where the shaft is rotating inside the stationary bearing (bush). They are separated with a small clearance space filled with lubricant to minimize friction and wear. Journal bearings are widely used in many applications such as cars and trains. Furthermore, journal bearing is used in high-speed rotating machines such as compressors, gas turbines, water turbines, steam turbines, electric generators and others.

In the journal bearing, there is a relatively small is placement called eccentricity between the center of the shaft and the center of bearing. The pressure distribution and the amount of load depend on this the value of the eccentricity. The minimum film thickness in a hydrodynamically lubricated bearing, which also depends on the eccentricity, is a function of the applied load [1]. The determination of static and dynamic characteristics of finite length misaligned journal bearings is considered as an important subject in the designing of such type of bearings. Therefore, this topic has drawn the attention of the researchers in order to improve the bearing performance. Lund and Thomsen [2] used a numerical method for solving Reynolds equation by finite difference method to calculate the static and the dynamic characteristics of journal bearing with based on Reynolds boundary conditions for a length to diameter ratio of L/D =0.5 and 1. Maspeyrot and Frene [3] presented a numerical analysis of journal misalignment problem under high load. Yucel [4] calculated the dynamic characteristics of a short journal bearing based on the use of analytical solution of the Reynolds equation. Zhao et al. [5] proposed that both stability and oil film forces of the hydrodynamic bearing can be expressed by using linear oil film coefficients. Ionescu [6] suggested a new mathematical model for analytical solution of thermo-hydrodynamic lubrication to make a quick estimation of the main parameters for finite length journal bearings. Chasalevris and Sfyris [7] proposed a new analytical method to find a solution for Reynolds equation in order to obtain the static and dynamic characteristics of the finite length journal bearing. Kumar et al. [8] used analytical solution to investigate the performance of the hydrodynamic bearings for short bearing only. Xu et al. [9] presented a solution for the static and dynamic characteristics of journal bearing considering the influence of thermohydrodynamic and turbulent flow. Jang and Khonsari [10] showed in a review paper that at heavy load, the misalignment significantly affects the system performance. Feng et al. [11] presented a solution of water-lubricated journal bearing by using a misaligned thermodynamic (THD) model with a turbulent flow consideration. They recommended the studying of these two effects on dynamic coefficients, particularly at high eccentricity ratio and rotary speed. Jamil et al. [2] used analytical solution for short journal bearing to calculate the

`

dynamic coefficients of a rotor supported on a worn journal bearing. Zhang et al. [13] presented an efficient method for water-lubricated circular journal bearing with different working conditions and bearing geometries to determine the force and stiffness coefficients of bearing. Binu et al., [14] developed a new test rig to obtain experimentally the hydrodynamic pressure for finite journal bearings. The results obtained by building a software revealed that the difference between the experimental maximum pressure and theoretical solution was about 20%. Zhang et al. [15] analyzed hydrodynamic water lubrication of a circular journal bearing under misaligned effect to select proper design parameters for the bearing. The obtained results showed a decrease in the load-carrying capacity of the bearing due to misalignment. Tarasevych et al. [16] studied the effect of random change of main geometrical parameters of full journal bearings using a mathematical model. Jamali and Al-Hamood [17] used a 3D model to evaluate the misalignment effect without considering the dynamic coefficients. Dyk et al. [18] introduced an approximate solution of the Reynolds equation of finite-length journal bearings to specify the linear dynamic coefficients and stability of the system. The researchers used a numerical approach but under the assumption of the Gumble boundary condition (π –film boundary condition).

This paper presents a solution to the problem of misaligned journal bearing using a 3D misalignment model in order to calculate the static and dynamic characteristics of the system using Reynolds boundary condition method. Finite length bearings are considered in the analyses where such range of length to diameter ratio is commonly used in the industry.

2.Basic Equations

The basic equations for the problem of journal bearing are Reynolds equations and film thickness equation which are given by [17] and [7]:

$$\frac{\partial}{\partial x}\left(\frac{\rho h^3}{12\eta}\frac{\partial p}{\partial x}\right)+\frac{\partial}{\partial z}\left(\frac{\rho h^3}{12\eta}\frac{\partial p}{\partial z}\right)=U_m\frac{\partial \rho h}{\partial x}+\frac{\partial \rho h}{\partial t} \tag{1}$$

Where,

$U_m = \frac{U_j+U_b}{2}$, U_m is the mean velocity of two surfaces,

The bearing is fixed which means $U_{b=0}$, and

$\frac{\partial p}{\partial x}$ = the pressure gradient in circumferential direction.

`

$\frac{\partial p}{\partial z}$ = the pressure gradient in axial direction

$\frac{\partial h}{\partial x}$ = the wedge action term

$\frac{\partial h}{\partial t}$ = the squeeze term

Reynolds' equation is considered as one of the complicated non-linear partial differential equations. Several hypotheses have been formulated and simplified in order to obtain a suitable solution for this equation. This includes an incompressible flow assumption (ρ = constant) and for the steady-state case, the squeeze term is considered zero ($\frac{\partial h}{\partial t} = 0$). Therefore, Eq. (1), can be written as:

$$\frac{\partial}{\partial x}\left(\frac{h^3}{\eta}\frac{\partial p}{\partial x}\right)+\frac{\partial}{\partial z}\left(\frac{h^3}{\eta}\frac{\partial p}{\partial z}\right)=6U\frac{\partial h}{\partial x} \tag{2}$$

The oil film thickness equation is given by [17]:

$$h=c(1+\varepsilon_r\cos\theta) \tag{3}$$

Therefore, using dimensionless presentation, Eq. (2), becomes

$$\frac{\partial}{\partial\theta}\left(H^3\frac{\partial P}{\partial\theta}\right)+\alpha\frac{\partial}{\partial Z}\left(H^3\frac{\partial P}{\partial Z}\right)-\frac{\partial H}{\partial\theta}=0 \tag{4}$$

Where:

$\alpha = \frac{R^2}{L^2} = \frac{1}{4(\mathrm{L/D})^2}$

Similarly Eq. (3), is,

$$H=\left(1+\varepsilon_r\cos\theta\right) \tag{5}$$

Where:

$$X=R\theta, Z=\frac{z}{L}, H=\frac{h}{c}$$

$$U=R\omega, P=\frac{p-p_0}{6\eta\omega}\left(\frac{c}{R}\right)^2$$

3.3D misalignment in journal bearing

`

The 3D model for the misalignment is illustrated schematically in Fig. 1, The deviations in the vertical and horizontal directions are given by Δ_v and Δ_h, respectively.

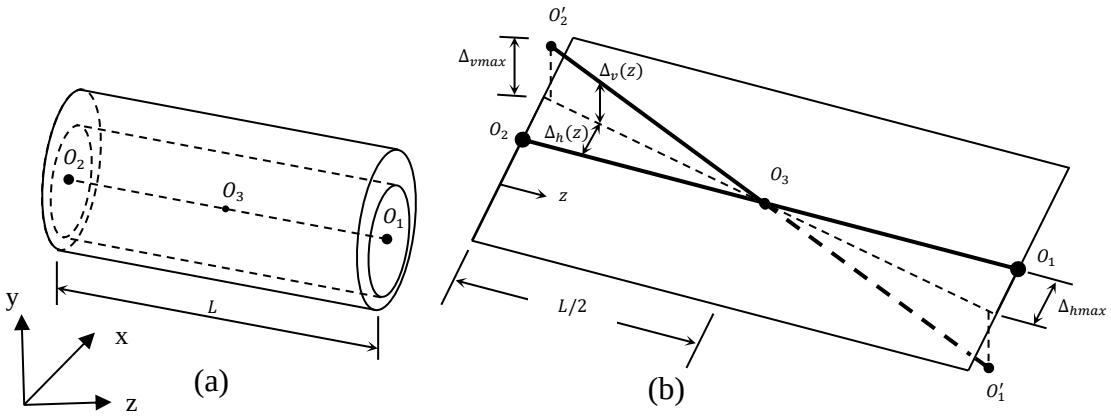

Figure 1. Journal bearing model. (a) 3D journal bearing; (b) axes deviations [17].

Figure 2. shows the deviations at any section for the two halves of the bearing. Figure 2a. illustrates the left side of the bearing ($z \leq L/2$) and Fig. 2b, shows the bearing right side ($z > L/2$).

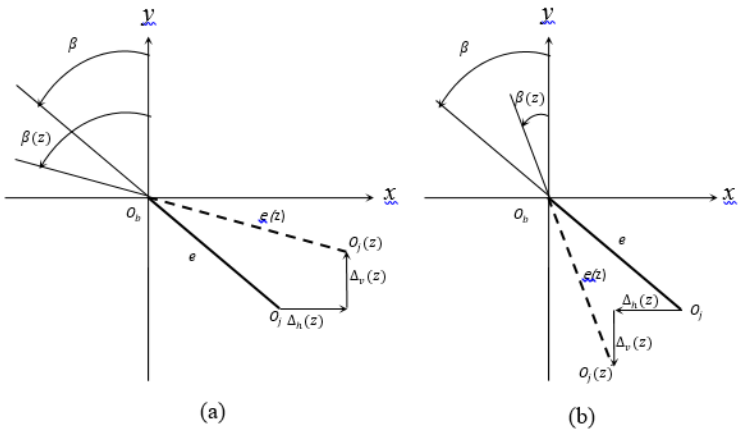

Figure 2. Deviation of the journal center due to misalignment; (a) ($z \leq L/2$);
(b) ($z > L/2$) [17].

`

It can be easily derived the following dimensionless equations which represent the misalignment at any given axial position (z):

$$\left.\begin{aligned} \delta_v(Z) &= \delta_{v\max}(1-2Z) \ for Z \le 1/2 \\ \delta_v(Z) &= \delta_{v\max}(2Z-1) \ for Z > 1/2 \\ \delta_h(Z) &= \delta_{h\max}(1-2Z) \ for Z \le 1/2 \\ \delta_h(Z) &= \delta_{h\max}(2Z-1) \ for Z > 1/2 \end{aligned}\right\} \quad (6)$$

Where $\delta = \frac{\Delta}{c}$

$$for Z \le 1/2$$

$$\varepsilon_r(Z) = \sqrt{(\varepsilon_r \cos\beta - \delta_v(Z))^2 + (\varepsilon_r \sin\beta + \delta_h(Z))^2} \quad (7)$$

$$\beta(Z) = Arc\tan\frac{\varepsilon_r \sin\beta + \delta_h(Z)}{\varepsilon_r \cos\beta - \delta_v(Z)} \quad (8)$$

$$for Z > 1/2$$

$$\varepsilon_r(Z) = \sqrt{(\varepsilon_r \cos\beta + \delta_v(Z))^2 + (\varepsilon_r \sin\beta - \delta_h(Z))^2} \quad (9)$$

$$\beta(Z) = Arc\tan\frac{\varepsilon_r \sin\beta - \delta_h(Z)}{\varepsilon_r \cos\beta + \delta_v(Z)} \quad (10)$$

The oil film thickness varies along the axial direction because the eccentricity is not constant along this-direction in case of misalignment. Therefore, the equation of film thickness for misaligned journal bearing is,

$$H(\theta, Z) = (1 + \varepsilon_r(Z)\cos\theta) \quad (11)$$

4. Bearing Characteristics

Swift-Stieber (Reynolds) Boundary Condition is used to calculate characteristics of bearing as it is a most realistic method for pressure evaluation which involves an iterative procedure to determine the boundary where the pressure and its gradient in the circumferential direction become zero.

4.1. Static characteristic: The considered static characteristics are: load-carrying capacity, attitude angle and Sommerfeld number. The load components in the radial direction (along the line of the center) [7] can be expressed in dimensionless form as:

$$\overline{W_r} = \int_0^1 \int_0^{\theta_c} P\cos\theta \, d\theta \, dZ \quad , \quad \overline{Wt} = \int_0^1 \int_0^{\theta_c} P\sin\theta \, d\theta \, dZ$$

`

$$\overline{W} = \sqrt{\overline{Wr}^2 + \overline{Wt}^2} \qquad (12)$$

Where,

$$\overline{W} = \frac{w}{6\eta\omega R L}\left(\frac{c}{R}\right)^2$$

The attitude angle can be given by:

$$\beta = \tan^{-1}\left(\frac{Wt}{Wr}\right) \qquad (13)$$

The operating conditions of a journal bearing of aspect ratio L/D can be characterized using a single dimensionless parameter. An expression which defines the Sommerfeld number can be written by:

$$s = \frac{\eta N_r D L}{w}\left(\frac{R}{c}\right)^2 = \frac{1}{(6\pi\overline{W})} \qquad (14)$$

4.2. Dynamic characteristics:

Dynamic characteristics considered eight Dynamic coefficients are considered in this work. Four coefficients for the stiffness and the other coefficients are for the damping. These coefficients are customarily denoted by (k_{xx}, k_{xy}, k_{yx}, k_{yy}, b_{xx}, b_{xy}, b_{yx}, b_{yy}). The coordinate system defined by [2] is used in the calculation of these coefficients which is illustrated in Fig. 3, where x_0, y_0 is steady-state position of the journal center.

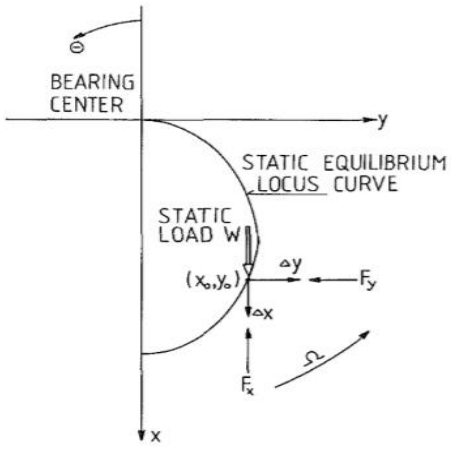

Figure 3. Coordinate system for dynamic characteristics (Lund, 1987)[2].

`

In this section, equations of the dynamic coefficients are derived based on the solution of Reynolds Eq. (1), which can be used in order to calculate stiffness and damping coefficients of finite-length journal bearing.

$$\frac{\partial}{\partial x}\left(\frac{h^3}{12\eta}\frac{\partial p}{\partial x}\right)+\frac{\partial}{\partial z}\left(\frac{h^3}{12\eta}\frac{\partial p}{\partial z}\right)=\frac{U}{2}\frac{\partial h}{\partial x}+\frac{\partial h}{\partial t} \tag{15}$$

The equation of film thickness under dynamic condition is [2]:

$$h = h_0 + \Delta x\cos\theta + \Delta y\sin\theta \tag{16}$$

The differentiation of this equation with respect to time yields,

$$\frac{\partial h}{\partial t} = \Delta\dot{x}\cos\theta + \Delta\dot{y}\sin\theta \tag{17}$$

Substituting of this equation into Eq. (15), and using dimensionless forms yields,

$$\frac{\partial}{\partial\theta}\left(H^3\frac{\partial P}{\partial\theta}\right)+\alpha\frac{\partial}{\partial Z}\left(H^3\frac{\partial P}{\partial Z}\right)=\frac{\partial H}{\partial\theta}+2\Delta\dot{X}\cos\theta+2\Delta\dot{Y}\sin\theta \tag{18}$$

Where,

$$\dot{X}=\frac{R\dot{x}}{Uc},\dot{Y}=\frac{R\dot{y}}{Uc}$$

The resultant force can be expressed using x and y coordinates of the journal center and the velocity components ($\dot{x}.\dot{y}$) as:

$$F_x=\int_0^1\int_0^{\theta_c}P\cos\theta d\theta dZ \qquad F_y=\int_0^1\int_0^{\theta_c}P\sin\theta d\theta dZ \tag{19}$$

Where the resultant force is,

$$F=\sqrt{{F_x}^2+{F_y}^2} \tag{20}$$

The coefficients (stiffness and damping) can be written in the following form of equations [19]:

`

$$[k]=\begin{bmatrix} k_{xx} & k_{xy} \\ k_{yx} & k_{yy} \end{bmatrix}=\begin{bmatrix} \frac{\partial F_x}{\partial X} & \frac{\partial F_x}{\partial Y} \\ \frac{\partial F_y}{\partial X} & \frac{\partial F_y}{\partial Y} \end{bmatrix} \tag{21}$$

$$[b]=\begin{bmatrix} b_{xx} & b_{xy} \\ b_{yx} & b_{yy} \end{bmatrix}=\begin{bmatrix} \frac{\partial F_x}{\partial \dot{X}} & \frac{\partial F_x}{\partial \dot{Y}} \\ \frac{\partial F_y}{\partial \dot{X}} & \frac{\partial F_y}{\partial \dot{Y}} \end{bmatrix} \tag{22}$$

Therefore, differentiation of Eq. (1), based on Eq. (21) and (22), gives:

$$\begin{aligned} k_{xx} &= \int_0^1 \int_0^{2\pi} \left(\frac{\partial P}{\partial X} \right) \cos\theta \, d\theta dz \\ k_{xy} &= \int_0^1 \int_0^{2\pi} \left(\frac{\partial P}{\partial Y} \right) \cos\theta d\theta dz \\ k_{yx} &= \int_0^1 \int_0^{2\pi} \left(\frac{\partial P}{\partial X} \right) \sin\theta \, d\theta dz \\ k_{yy} &= \int_0^1 \int_0^{2\pi} \left(\frac{\partial P}{\partial Y} \right) \sin\theta \, d\theta dz \end{aligned} \tag{23}$$

The stiffness coefficients can be written in the following form for the purpose of consistency with reference [2]:

$$\begin{aligned} K_{xx} &= \frac{ck_{xx}}{F}, K_{xy} = \frac{ck_{xy}}{F} \\ K_{yx} &= \frac{ck_{yx}}{F}, K_{yy} = \frac{ck_{yy}}{F} \end{aligned} \tag{24}$$

Also, in the same way, the damping coefficients are calculated from using the integration over the solution domain for the pressure derivatives with respect to $\dot{X}$ and $\dot{Y}$ as:

`

$$b_{xx} = \int_0^1 \int_0^{2\pi} \left(\frac{\partial P}{\partial \dot{X}} \right) \cos\theta \, d\theta dz$$
$$b_{xy} = \int_0^1 \int_0^{2\pi} \left(\frac{\partial P}{\partial \dot{Y}} \right) \cos\theta d\theta dz$$
$$b_{yx} = \int_0^1 \int_0^{2\pi} \left(\frac{\partial P}{\partial \dot{X}} \right) \sin\theta d\theta dz$$
$$b_{yy} = \int_0^1 \int_0^{2\pi} \left(\frac{\partial P}{\partial \dot{Y}} \right) \sin\theta d\theta dz \qquad (25)$$

Similarly, the damping coefficients are given by,

$$B_{xx} = \frac{c\omega b_{xx}}{F}, B_{xy} = \frac{c\omega b_{xy}}{F}$$
$$B_{yx} = \frac{c\omega b_{yx}}{F}, B_{yy} = \frac{c\omega b_{yy}}{F} \qquad (26)$$

It can be seen that from the previous equations, to calculate $K_{xx}, K_{xy}, K_{yx}, K_{yy}, B_{xx}, B_{xy}, B_{xy}, B_{yx}, B_{yy}$. The evaluation of the derivatives $\frac{\partial \mathrm{P}}{\partial \mathrm{X}}$, $\frac{\partial \mathrm{P}}{\partial \mathrm{Y}}, \frac{\partial \mathrm{P}}{\partial \dot{\mathrm{X}}}$ and $\frac{\partial \mathrm{P}}{\partial \dot{\mathrm{Y}}}$ are required based on the use of Reynolds equation. Therefore, the derivatives are evaluated by differentiation of Eq. (18), which yields,

$$\frac{\partial}{\partial\theta}\left(H^3 \frac{\partial P_x}{\partial\theta} \right) + \alpha \frac{\partial}{\partial Z}\left(H^3 \frac{\partial P_x}{\partial Z} \right) = -\frac{\partial}{\partial\theta}\left(3H^2 \cos\theta \frac{\partial P}{\partial\theta} \right) - \alpha \frac{\partial}{\partial Z}\left(3H^2 \cos\theta \frac{\partial P}{\partial Z} \right) - \sin\theta \qquad (27)$$

Also, the differentiation with respect to Y, gives:

$$\frac{\partial}{\partial\theta}\left(H^3 \frac{\partial P_y}{\partial\theta} \right) + \alpha \frac{\partial}{\partial Z}\left(H^3 \frac{\partial P_y}{\partial Z} \right) = -\frac{\partial}{\partial\theta}\left(3H^2 \sin\theta \frac{\partial P}{\partial\theta} \right) - \alpha \frac{\partial}{\partial Z}\left(3H^2 \sin\theta \frac{\partial P}{\partial Z} \right) + \cos\theta$$

(28)

Similarly, the differentiation of Eq. (18), with respect to $\dot{X}$ and $\dot{Y}$ respectively, gives:

$$\frac{\partial}{\partial\theta}\left(H^3 \frac{\partial P_{\dot{x}}}{\partial\theta} \right) + \alpha \frac{\partial}{\partial Z}\left(H^3 \frac{\partial P_{\dot{x}}}{\partial Z} \right) = \cos\theta \qquad (29)$$

(30)

$$\frac{\partial}{\partial\theta}\left(H^3 \frac{\partial P_{\dot{y}}}{\partial\theta} \right) + \alpha \frac{\partial}{\partial Z}\left(H^3 \frac{\partial P_{\dot{y}}}{\partial Z} \right) = \sin\theta$$

`

5. Numerical analysis

The numerical form for Eq. (4), will be explained below using the discretization shown in Fig. 4,

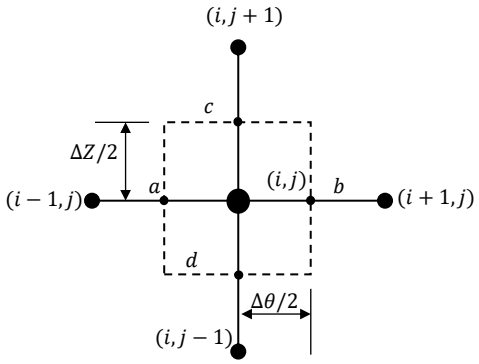

Figure 4. Finite difference discretization

$$\frac{\partial H}{\partial \theta} = \frac{H_{(i+1,j)} - H_{(i-1,j)}}{2\Delta\theta} \tag{31}$$

$$\frac{\partial}{\partial \theta}\left(H^3 \frac{\partial P}{\partial \theta}\right) = \frac{H^3 \left.\frac{\partial P}{\partial \theta}\right|_b - H^3 \left.\frac{\partial P}{\partial \theta}\right|_a}{\Delta\theta} \tag{32}$$

$$\left.\frac{\partial P}{\partial \theta}\right|_b = \frac{P_{(i+1,j)} - P_{(i,j)}}{\Delta\theta} \tag{32a}$$

$$\left.\frac{\partial P}{\partial \theta}\right|_a = \frac{P_{(i,j)} - P_{(i-1,j)}}{\Delta\theta} \tag{32b}$$

$$H_b^3 = \left[\frac{H(i+1,j) + H(i,j)}{2}\right]^3 \tag{32c}$$

$$H_a^3 = \left[\frac{H(i,j) + H(i-1,j)}{2}\right]^3 \tag{32d}$$

`

Similarly, the gradient in the Z direction can be written in the same way that used in the circumferential direction. After that Substituting these equations in Eq. (4), and solving for $P(i,j)$ yields:

$$P_{(i,j)}=\frac{1}{\gamma}\left[H_b{}^3\,P_{(i+1,j)}+H_a{}^3\,P_{(i-1,j)}+\alpha C_2 H_C{}^3\,P_{(i,j+1)}+\alpha C_2 H_d{}^3\,P_{(i,j-1)}-C_1 H_{(i+1,j)+}C_1 H_{(i-1,j)}\right] \tag{33}$$

Where:

$$\alpha=\frac{R^2}{L^2},\ C_1=\frac{\Delta\theta}{2},\ C_2=\frac{(\Delta\theta)^2}{(\Delta Z)^2}$$
$$\gamma=H_b^3+H_a^3+\alpha C_2 H_c^3+\alpha C_2 H_d^3$$

The numerical form for oil film thickness is,

$$H(i,j)=\left(1+\varepsilon_r\cos\theta_{(i,j)}\right) \tag{34}$$

The determination of the dynamic characteristics requires the numerical solution of Eq. (27), (28), (29) and (30). A similar procedure that used for the steady-state case is adopted to obtain the solution of these equations which can be written in a general form. Therefore, RHS (27) in a numerical form becomes,

$$\frac{(3\cos\theta_a H_a^2+3\cos\theta_b H_b^2)P_{(i,j)}}{(\Delta\theta)^2}-\frac{3\cos\theta_a H_a^2 P_{(i+1,j)}}{(\Delta\theta)^2}-\frac{3\cos\theta_b H_b^2 P_{(i-1,j)}}{(\Delta\theta)^2}+$$
$$\alpha\frac{(3\cos\theta_d H_d^2+3\cos\theta_c H_c^2)P_{(i,j)}}{(\Delta Z)^2}-\alpha\frac{3\cos\theta_d H_d^2 P_{(i,j+1)}}{(\Delta Z)^2}-\alpha\frac{3\cos\theta_c H_c^2 P_{(i,j-1)}}{(\Delta Z)^2}-\sin\theta \tag{35}$$

A similar procedure can be used to discretize the right-hand sides of the other equations and therefore these right-hand sides can be written in discrete forms as:

RHS (28) =

$$\frac{\left(3\sin\theta_a H_a^2+3\sin\theta_b H_b^2\right)P_{(i,j)}}{(\Delta\theta)^2}-\frac{3\sin\theta_a H_a^2 P_{(i+1,j)}}{(\Delta\theta)^2}-\frac{3\sin\theta_b H_b^2 P_{(i-1,j)}}{(\Delta\theta)^2}+$$
$$\alpha\frac{\left(3\sin\theta_d H_d^2+3\sin\theta_c H_c^2\right)P_{(i,j)}}{(\Delta Z)^2}-\alpha\frac{3\sin\theta_d H_d^2 P_{(i,j+1)}}{(\Delta Z)^2}-\alpha\frac{3\sin\theta_c H_c^2 P_{(i,j-1)}}{(\Delta Z)^2}+\cos\theta \tag{36}$$

`

$$RHS(31) = cos\theta_{(i,j)} \tag{37}$$

$$RHS(32) = sin\theta_{(i,j)} \tag{38}$$

Now using Eq. (35), (36), (37) and (38), Eq. (33), can be solved numerically to calculate the corresponding pressure derivative. Therefore, the dynamic characteristics (stiffness and damping coefficients) can now be determined by,

$$\begin{aligned} K_{xx} &= \sum_{j=1}^{M}\sum_{i=1}^{N}\left(\frac{\partial P(i,j)}{\partial X}\right)\cos\theta\Delta\theta\Delta Z \\ K_{xy} &= \sum_{j=1}^{M}\sum_{i=1}^{N}\left(\frac{\partial P(i,j)}{\partial Y}\right)\cos\theta\Delta\theta\Delta Z \\ K_{yx} &= \sum_{j=1}^{M}\sum_{i=1}^{N}\left(\frac{\partial P(i,j)}{\partial X}\right)\sin\theta\Delta\theta\Delta Z \\ K_{yy} &= \sum_{j=1}^{M}\sum_{i=1}^{N}\left(\frac{\partial P(i,j)}{\partial Y}\right)\sin\theta\Delta\theta\Delta Z \end{aligned} \tag{39}$$

$$\begin{aligned} B_{xx} &= \sum_{j=1}^{M}\sum_{i=1}^{N}\left(\frac{\partial P(i,j)}{\partial \dot{X}}\right)\cos\theta\Delta\theta\Delta Z \\ B_{xy} &= \sum_{j=1}^{M}\sum_{i=1}^{N}\left(\frac{\partial P(i,j)}{\partial \dot{Y}}\right)\cos\theta\Delta\theta\Delta Z \\ B_{yx} &= \sum_{j=1}^{M}\sum_{i=1}^{N}\left(\frac{\partial P(i,j)}{\partial \dot{X}}\right)\sin\theta\Delta\theta\Delta Z \\ B_{yy} &= \sum_{j=1}^{M}\sum_{i=1}^{N}\left(\frac{\partial P(i,j)}{\partial \dot{Y}}\right)\sin\theta\Delta\theta\Delta Z \end{aligned} \tag{40}$$

6. Results

6.1 Effect of mesh density

The total number of mesh points that required to be used in the solution in both directions is examined using 50 to 25600 points and it is observed that the results for the aligned and misaligned cases are sufficient enough when $k = 16471$.

`

6.2 Verification of misaligned model:

A comparison between the geometrical model of 3D misalignment that used in this work and the results of a recent reference [9] is performed in this section. They presented a study with and without the effect of thermodynamic and turbulent flow on the misaligned journal bearing. The validation performed with the later case in which the oil film thickness was determined by the use of the following equation:

$$h = c + e_o \cos(\theta - \varphi_o) + e'(\frac{z}{D} - \frac{1}{2})\cos(\theta - \alpha - \varphi_o)$$

In the current work, another expression for the equation of oil film thickness is derived where it is a function of the eccentricity ratio of journal bearing and it is variable along the axial direction. The results of several cases of both maximum horizontal and vertical deviations are shown in Fig. 5,. These Fig. 5a and 5b, illustrates a comparison between the two sets of results for three values of ($\delta_{hmax}, \delta_{vmax}$) as (0.2, 0.2) and (0.2, 0.3), respectively. It can be seen that very close results have been obtained where the maximum difference for the three cases is less than 0.007%.

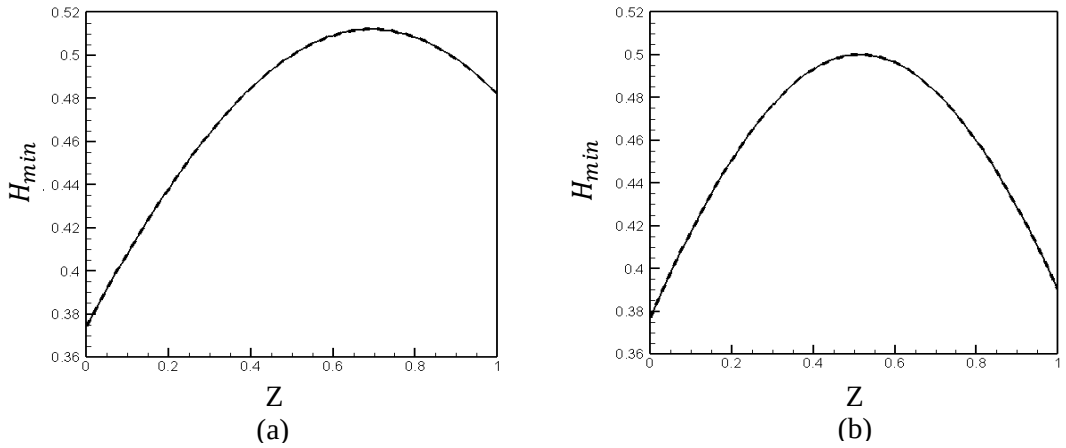

Figure 5. Comparison between current work and reference [9] for the min. film thickness. solid : reference , dashed : current .(a) δ_{hmax}= δ_{vmax}= 0.2, (b) δ_{hmax}=0.2, δ_{vmax}=0.3.

6.3 Verification of dynamic coefficients

The dynamic coefficients obtained in the current work are compared with the results of the well-known work of Lund and Thomsen [2]. The position of grooves relative to the line of the center is determined by the secant method [20]. The two sets of results are compared using a wide range of eccentricity ratio as shown in Fig. 6 and 7,

`

Figure 6. presents the results for (L/D=0.5) and Fig. 7, shows the results for (L/D=1). It has been found that the difference is less than 3 percent when the value of eccentricity ratio $\varepsilon_r < 0.5$ and less than 1 percent when the eccentricity ratio $\varepsilon_r \geq 0.5$. This result is satisfactory since the most practical

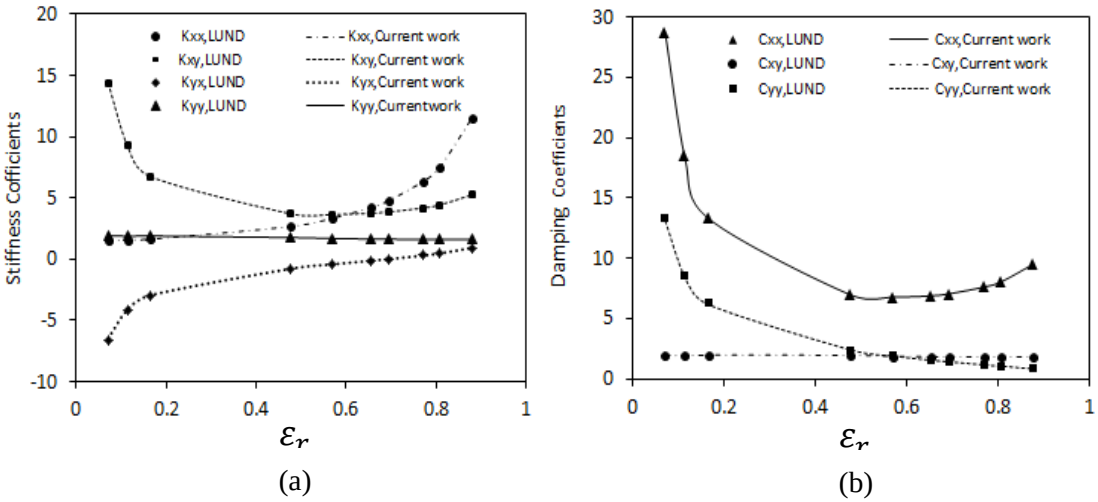

Figure 6. Comparison between the current work and [2] for the dimensionless dynamic coefficients, L/D=0.5. (a) stiffness coefficients;(b) damping coefficients.

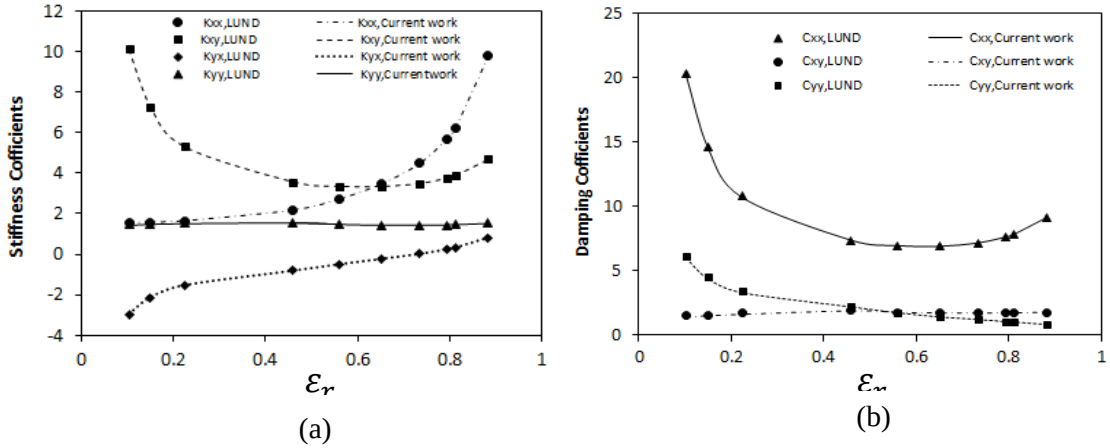

Figure 7. Comparison between the current work and [2] for the dimensionless dynamic coefficients, L/D=1. (a) stiffness coefficients; (b) damping coefficients.

6.4 Static characteristics

6.4.1 Effect of L/D and eccentricity ratios on the load-carrying capacity.

`

In this section, the load is determined by using different values of length to diameter and eccentricity ratios for the aligned case as illustrated in Fig. 8,. Figure 8a. Shows that the load is affected by the L/D ratio where it is calculated for a wide range of (L/D) ratio changes from (0.25 to 2.5) in a step of 0.25. The results demonstrate that the load becomes larger for the high value of L/D ratio where the amount of load is 0.049 for L/D=0.25 and 0.912 when L/D=2.5. These results are calculated for an eccentricity ratio of 0.6. Figure 8b. illustrated the load variation with the eccentricity ratio for a finite length bearing where L/D=1.5. The range of eccentricity ratio is between 0.4 and 0.95. It can be seen that the load is significantly depending on the eccentricity ratio. The load varies from 0.333 when the eccentricity ratio is 0.4 to 7.014 for the eccentricity ratio of 0.95.

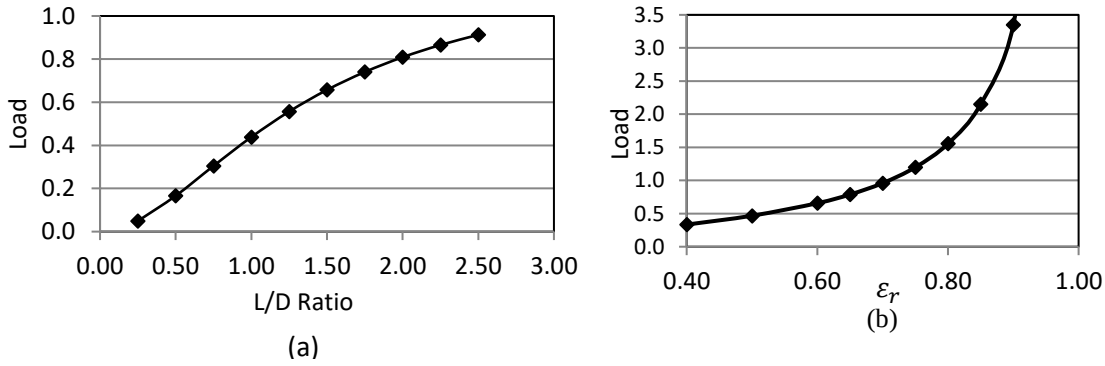

Figure 8. Effect of (L/D) and ε_r ratios on the load. (a) L/D ratio ($\varepsilon_r = 0.6$); (b) ε_r (L/D=1.5)

6.4.2 Effect of misalignment on the Attitude Angle and eccentricity ratio.

Figure 9. illustrates the effect of 3D misalignment on the eccentricity ratio and attitude angle. Figure 9a. shows the effect on the eccentricity ratio and Fig. 9b, illustrates the effect on the attitude angle. The results at the midplane correspond to the aligned case. It can be seen that the misalignment has a significant influence on ε_r and β where the change is clear along the axial direction.

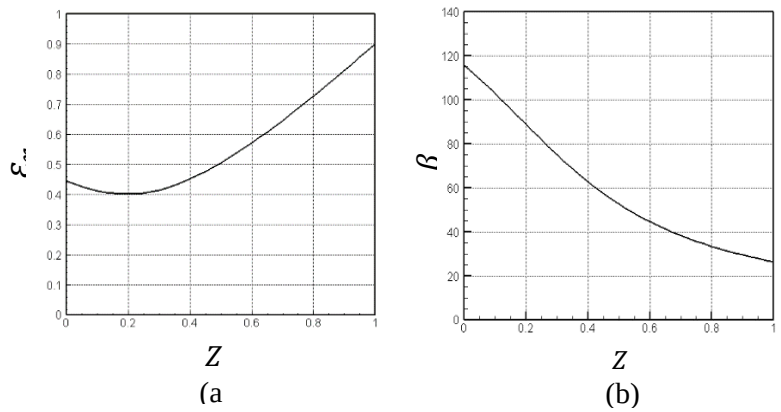

Figure 9. Effect of 3D misalignment ($\delta_{vmax} = 0.5, \delta_{hmax} = 0$) for L/D=2 on the eccentricity ratio and attitude angle along the Z-axis. (a) Eccentricity ratio (ε_r); (b) Attitude angle (β).

`

6.4.3 Effect of the severe 3D misalignment on the maximum pressure and the minimum filmthickness.

The effect of 3D misalignment (vertical and horizontal) on P_{max} and H_{min}, which have influences on the performance of the journal bearing, is shown in Figure 10. The results are calculated for a wide range of $\delta_{hmax}, \delta_{vmax}$ in a step of 0.1. Figure 10. shows the effect of 3D misalignment on P_{max} and H_{min} when (L/D=2). Regarding this figure, the 3D misalignment increases P_{max} significantly and decreases H_{min} particularly when $\delta_{hmax}, \delta_{vmax}$ >0.3. The maximum pressure increases from 0.8581 for the aligned case to 1.4392 when $\delta_{hmax}, \delta_{vmax}$= 0.54. The corresponding film thickness decreases from 0.3999 to 0.0827. This represents an increase of 67.7% in P_{max} and a reduction of 79.3% in H_{min}.

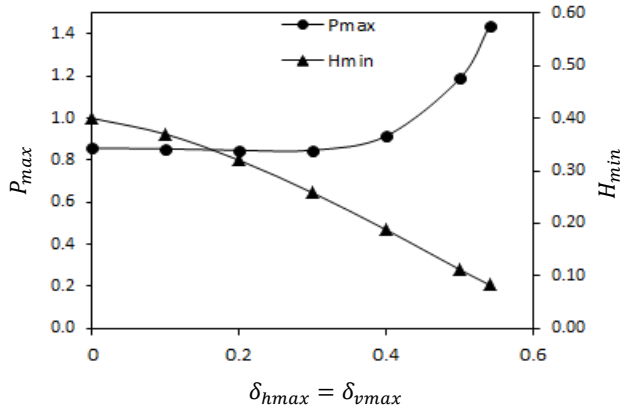

Figure 10. Effect 3D mis. (δ_{hmax} and δ_{vmax}) on the dimensionless max. pressure and min. thickness of the lubricant (L/D=2).

Two cases are considered in this section which are perfectly aligned and misaligned. 2D and 3D pressure distributions for (L/D=2) are shown in Fig. 11,. The left side shows the 2D pressure distribution and the right side shows the 3D pressure distribution for these cases, respectively. The maximum pressure for the first case (aligned) is (P_{max} =0.8581), while in the second case (misaligned), a significant change can be seen in the pressure distribution where (P_{max} = 1.4392). It can be seen in these figures that the misalignment causes pressure spike at a location very close to the edge.

`

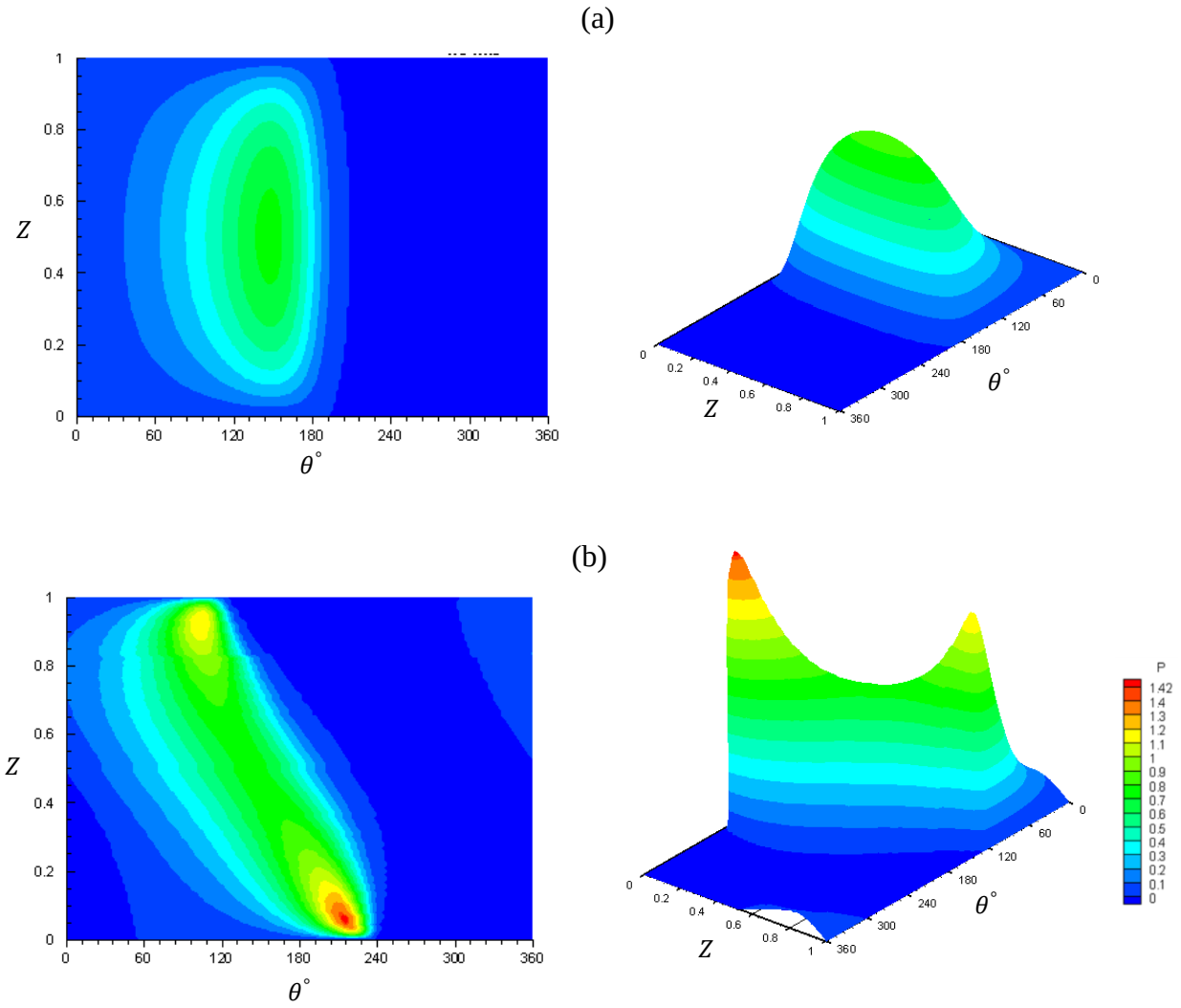

Figure 11.2D and 3D pressure distribution, L/D=2, $\delta_{hmax} = \delta_{vmax}$ =0.54; left :2D ,right: 3D, a:aligned,b: misaligned.

6.5 Dynamic coefficients

The effects of 3D misalignment on the dynamic coefficients ($K_{xx}, K_{xy}, K_{yx}, K_{yy}, B_{xx}, B_{xy}, B_{yx}, B_{yy}$) for L/D = 2 are shown in Table 1 for a range of misalignment values. The first row shows the result of the perfectly aligned case. It can be seen that the 3D misalignment has significant effects on these coefficients. The results show that K_{xx} is 1.8055 in the aligned case and increases to 2.4947 at the high level of misalignment. This means that the amount of change in K_{xx} in the case of 3D misalignment is 38.2% in comparison with the aligned case. The other stiffness coefficient K_{xy} is 2.6528 in the aligned case and decreases to 2.2874 in misaligned case. In such range, the percentage change in K_{xy} is 13.8%. The percentage change in

`

K_{yx} and K_{yy} is -241.2% and 81.1% respectively due to misalignment. Table 1. illustrates also the corresponding results for the dimensionless damping coefficients. It can be seen that B_{xx} is slightly affected by the misalignment. The variation is only 5.7% in comparison with the aligned case. The change in the other coefficients, B_{xy} $(= B_{yx})$, B_{yy} is 70.8 % and 78.1% respectively.

Table1. Effect of 3D misalignment on the stiffness and damping coefficients (L/D=2)

$\frac{\delta_{vmax}}{\delta_{hmax}} =$	K_{XX}	K_{XY}	K_{YX}	K_{YY}	B_{XX}	B_{XY}	B_{YX}	B_{YY}
0	1.805	2.653	-0.531	1.605	5.517	1.746	1.746	2.295
0.4	1.963	2.583	-0.979	2.019	5.581	1.238	1.238	3.067
0.45	2.057	2.528	-1.171	2.213	5.623	1.051	1.051	3.347
0.54	2.495	2.287	-1.811	2.906	5.832	0.509	0.509	4.088

7. Conclusions

In this paper, a detailed investigation is presented for the effect of misalignment on the characteristics of journal bearing. The governing equations are solved numerically for a finite length journal bearing based on the finite difference method where Reynolds boundary conditions method is used in the solution scheme. All the equations are presented in a dimensionless form for the purpose of generality of the results. A general 3D model for the misalignment is used in this analysis where both horizontal and vertical deviations of the journal axis are taken into consideration. A comprehensive program computer code has been developed which has the ability to analyse the problem of misaligned journal bearing, regardless of the L/D ratio. The results revealed that the eccentricity ratio and attitude angle are significantly affected by the misalignment along the axial direction. In general, the presence of misalignment increases P_{max} and reduce H_{min}. Furthermore, it changes the shape of the pressure distribution significantly. The effect of misalignment on the friction coefficient is not significant and side flow value decreases in the misaligned case due to the decrease of film thickness. The calculations of dynamic coefficients in this study are performed for L/D =1.5 and it has been found that the misalignment causes significant variation in these coefficients. Further investigation is required in order to consider the thermal effect in the analyses which will be performed in future work.

`

References

[1] Hamrock B.J. Fundamentals of Fluid Film Lubrication. New York: McGraw-Hill, Inc; 1991.

[2] Lund J W, Thomsen K K. A Calculation Method and Data for the Dynamic Coefficients of Oil-Lubricated Journal Bearings. ASME New York 1978.

[3] Maspeyrot P, Frene J. Comparison between Aligned and Misaligned Bearings under Dynamic Loading in both Quasi-Static and Dynamic Misalignment. Leeds-Lyon symposium on tribology September 1990; 19–26.

[4] Yucel U. Calculation of Dynamic Coefficients for Fluid. J. of Engineering Sciences 2005; 335-343.

[5] Zhao SX, Zhou H, Meng G, Zhu J. Experimental Identification of Linear Oil-Film Coefficients using Least-Mean-Square Method in Time Domain. Journal of Sound and Vibration 2005; 809–825.

[6] Ionescu M. The Analytical Calculation of Journal Bearing Parameters by Means of the Finite Bearing Theory. Lubrication Science (July) 2011; 347–353.

[7] Chasalevris A, Sfyris D. Evaluation of the Finite Journal Bearing Characteristics, Using the Exact Analytical Solution of the Reynolds Equation. Tribology International. Elsevier 2013; 216–234.

[8] Kumar V D, Chand S, Pandey KN. Effect of Different Flow Regime on the Static and Dynamic Performance Parameter of Hydrodynamic Bearing. Procedia Engineering Elsevier 2013; 520–528.

[9] Xu G, Zhou J, Geng H, Lu M, Yang L, Yu L. Research on the Static and Dynamic Characteristics of Misaligned Journal Bearing Considering the Turbulent and Thermohydrodynamic Effects. Journal of Tribology 2015; 024504-1.

[10] Jang JY, Khonsari MM. On the Characteristics of Misaligned Journal Bearings. Lubricants 2015; 27–53.

[11] Feng H, Jiang S, Ji A. Investigation of the Static and Dynamic Characteristics of Water-Lubricated Hydrodynamic Journal Bearing Considering Turbulent,Thermohydrodynamic and Misaligned Effects. Tribology International. Elsevier Ltd 2018.

[12] Jamil AN, Ali AA , Mohammad T. Study the Dynamic Behavior of Rotor Supported on a Worn Journal Bearing. Journal of Engineering 2015; 1–18.

[13] Zhang X, Yin Z, Gao G, Li Z. Determination of Stiffness Coefficients of Hydrodynamic Water-Lubricated Plain Journal Bearings. Tribiology International. Elsevier 2015; 37–47.

[14] Binu KG, Yathish K, Mallya R, Shenoy BS, Rao DS, Pai R. Experimental Study of Hydrodynamic Pressure Distribution in Oil Lubricated Two-axial Groove Journal Bearing. Materials Today: Proceedings. Elsevier Ltd 2015; 3453–3462.

[15] Zhang X, Yin Z, Jiang D, Gao G, Wang Y, Wang X. Load Carrying Capacity of Misaligned Hydrodynamic Water-Lubricated Plain Journal Bearings with Rigid Bush Materials. Tribiology International. Elsevier 2016.

[16] Tarasevych Y, Savchenko I, Sovenko N. Influence of Technological Deviations on the Basic Operational Characteristics of Hydrodynamic Bearings. Materials Science and Engineerng 2017.

[17] Jamali HU, Al-Hamood A. A New Method for the Analysis of Misaligned Journal bearing. Tribology in Industry 2018; 213–224.

[18] Dyk S, Rendl J, Byrtus M, Smolik L. Dynamic Coefficients and Stability Analysis of Finite-Length Journal Bearings Considering Approximate Analytical Solutions of the Reynolds Equation. Tribology International. Elsevier Ltd 2018; 229–244.

[19] Someya T. Journal bearing databook, Springer-Verlag Berlin Heidelberg, 1989.

[20] Chapra S. C. and Canale R. P., Numerical Methods for Engineer.

Nomenclature

Symbol	Description	**Units**
$B_{xx.}B_{xy}$ $B_{yx.}B_{yy}$	Dimensionless damping coefficients	-
c	Bearing radial clearance	m
D	Diameter of shaft	m
e	Eccentricity of journal	m
F_x	Force in x-direction	N
F_y	Force in y-direction	N
F	Total Force	N
H	Non- dimensional oil film thickness, $H = \frac{h}{c}$	-
$H_{\min}$	Dimensionless Minimum Oil film thickness	-
h	Oil film thickness	m

`

k	Total number of mesh $k = M \times N$	-
$K_{xx.}K_{xy}$ $K_{yx.}K_{yy}$	Dimensionless Stiffness coefficients	-
L	Bearing length	m
M	Number of mesh point in the longitudinal direction (z)	-
N	Number of mesh point in the circumferential direction (θ)	-
N_r	Rotational speed	Rps
P	Non-dimensional oil film pressure, $P = \frac{p}{6\eta\omega}\left(\frac{c}{R}\right)^2$	-
$\bar{P}$	Derivative of pressure (dimensionless)	-
P_{max}	Non-dimensional maximum pressure	-
R	Bearing radius	m
RF	Relaxation factor	-
s	Somerfeld number	-
t	Time	Sec
U	Velocity	m/sec
U_m	Mean velocity	m/sec
W	Total Load carrying capacity	N
$\bar{W}_r$	Dimensionless Load in the radial-direction	N
$\bar{W}_t$	Dimensionless Load in the tangential-direction	N
$\bar{W}$	Dimensionless total load of journal bearing	-
Z	Non-dimensional axial coordinate, $Z = \frac{z}{L}$	-
z	Axial coordinate, $0 \leq z \leq L$	m

`

Greek symbols

Symbol	Description	Units
α	Constant in Reynolds equation	-
β	Attitude angle	degree
Δ_h	Horizontal misalignment	m
Δ_{hmax}	Maximum horizontal misalignment	m
Δ_v	Vertical misalignment	m
Δ_{vmax}	Maximum vertical misalignment	m
$\Delta\theta$	Step in the circumferential direction	degree
ΔZ	Step in the longitudinal direction	-
δ	Dimensionless misalignment $\delta = \Delta/c$	-
ε_r	Eccentricity Ratio, $\varepsilon_r = \frac{e}{c}$	-
η	Lubricant viscosity	Pa. s
θ	Angle in the circumferential direction	degree
θ_c	Cavitation angle	degree
ρ	Density of oil	Kg/m^3
φ_d	Dimensionless side –leakage flow	-
ω	Journal Angular velocity, $\omega = 2\pi N$	rad/sec
f	Friction coefficient	-